

# Analysis of the Impact of Remote Oxygen Plasma Treatment on the Surface Chemistry and Electrochemical Properties of Graphite Felt Electrodes for Redox Flow Batteries

L. Mauricio Murillo-Herrera<sup>[a]\*</sup>, Carlos J. Mingo<sup>[a]</sup>, J. Obrero-Pérez<sup>[b]</sup>, Juan R. Sánchez-Valencia<sup>[b]</sup>, Michael W. Thielke<sup>[a]</sup>, Ángel Barranco<sup>[b]</sup>, Ana B. Jorge Sobrido<sup>[a]\*</sup>.

<sup>[a]</sup>School of Engineering and Materials Science. Queen Mary University of London. Mile End Rd, London E1 4NS, United Kingdom

<sup>[b]</sup>Instituto de Ciencia de Materiales de Sevilla. Consejo Superior de Investigaciones Científicas. c/Américo Vespucio 49, 41092, Sevilla, Spain.

## Table of contents

|  |    |
|--|----|
| <b>Table S1:</b> Deconvolution of High resolution XPS data.....  | 4  |
| <b>Table S2:</b> Raman analysis including Gaussian and Lorentzian contributions for each band..  | 7  |
| <b>Figure S1:</b> Pristine <b>GF</b> high resolution C1s & O1s spectra.  | 4  |
| <b>Figure S2:</b> <b>GF400</b> high resolution C1s & O1s spectra.  | 4  |
| <b>Figure S3:</b> Anomalous <b>GF400</b> high resolution C1s & O1s spectra.  | 5  |
| <b>Figure S4:</b> <b>P10s</b> high resolution C1s & O1s spectra.   | 5  |
| <b>Figure S5:</b> <b>P60s</b> high resolution C1s & O1s spectra.   | 6  |
| <b>Figure S6:</b> <b>P600s</b> high resolution C1s & O1s spectra.  | 6  |
| <b>Figure S7:</b> Pristine <b>GF</b> Raman spectrum and D/G band deconvolution.  | 8  |
| <b>Figure S8:</b> <b>GF400</b> Raman spectrum and D/G band deconvolution.  | 8  |
| <b>Figure S9:</b> <b>P10s</b> Raman spectrum and D/G band deconvolution.   | 8  |
| <b>Figure S10:</b> <b>P60s</b> Raman spectrum and D/G band deconvolution.  | 8  |
| <b>Figure S11:</b> <b>P600s</b> Raman spectrum and D/G band deconvolution.   | 9  |
| <b>Figure S12:</b> Pristine <b>GF</b> cyclic voltammetry showcasing non-faradaic current at different scan rates and linear fit of a current vs scan rate plot.....                    | 10 |
| <b>Figure S13:</b> <b>GF400</b> cyclic voltammetry showcasing non-faradaic current at different scan rates and linear fit of a current vs scan rate plot.                              | 10 |
| <b>Figure S14:</b> <b>P10s</b> cyclic voltammetry showcasing non-faradaic current at different scan rates and linear fit of a current vs scan rate plot.                               | 11 |
| <b>Figure S15:</b> <b>P60s</b> cyclic voltammetry showcasing non-faradaic current at different scan rates and linear fit of a current vs scan rate plot.                               | 11 |
| <b>Figure S16:</b> <b>P600s</b> cyclic voltammetry showcasing non-faradaic current at different scan rates and linear fit of a current vs scan rate plot.                              | 12 |
| <b>Figure S21:</b> Pore-size distributions from electrodes as derived from BET analysis.   | 13 |
| <b>Figure S22:</b> Schematic of a Single-electrolyte flow cell.  | 14 |
| <b>Figure S23:</b> Breakdown of impedance contributions: Ohmic resistance (Rs), charge-transfer resistance (Rct) and mass-transport resistance (Rmt) at 110 mL min <sup>-1</sup> ..... | 14 |
| <b>Figure S24:</b> Breakdown of impedance contributions: Ohmic resistance (Rs), charge-transfer resistance (Rct) and mass-transport resistance (Rmt) at 50 mL min <sup>-1</sup> .....  | 15 |
| <b>Figure S25:</b> Breakdown of impedance contributions: Ohmic resistance (Rs), charge-transfer resistance (Rct) and mass-transport resistance (Rmt) at 30 mL min <sup>-1</sup> .....  | 15 |
| <b>Figure S26:</b> Breakdown of impedance contributions: Ohmic resistance (Rs), charge-transfer resistance (Rct) and mass-transport resistance (Rmt) at 10 mL min <sup>-1</sup> .....  | 16 |
| <b>Figure S17:</b> Pressure drop plot from different electrodes showcasing curve hysteresis.....   | 17 |

**Figure S18:** Schematic of a Flow cell set up to perform pressure drop measurements. **Error! Bookmark not defined.**

**Figure S19:** Darcy-Forchheimer fitting..... 18

**Figure S20:** Permeability values derived from Darcy-Forchheimer fitting..... 18

| Chemical shift   | Gf pristine |         |         | Gf400   |      |         | Gf400 anomalous |         |         | P60s  |         |         | P60s    |         |       |
|------------------|-------------|---------|---------|---------|------|---------|-----------------|---------|---------|-------|---------|---------|---------|---------|-------|
|                  | Sample1     | Sample2 | Sample3 | Average | STD  | Sample1 | Sample2         | Sample3 | Average | STD   | Sample1 | Sample2 | Sample3 | Average | STD   |
| Cts              | 80.63       | 77.95   | 77.82   | 78.80   | 1.58 | 76.73   | 74.15           | 76.62   | 75.83   | 1.46  | 65.20   | 63.97   | 70.19   | 73.78   | 1.47  |
| C-C              | 7.24        | 8.41    | 7.51    | 7.72    | 0.61 | 7.22    | 6.06            | 6.93    | 6.74    | 0.60  | 13.41   | 9.98    | 6.99    | 3.09    | 4.69  |
| C-C low B/C/H    | 1.59        | 3.65    | 2.07    | 1.41    | 0.84 | 1.43    | 3.40            | 7.63    | 3.93    | 4.13  | 7.97    | 4.52    | 6.03    | 6.02    | 5.28  |
| C-C high B/Adv C | 0.60        | 0.70    | 1.49    | 0.93    | 0.49 | 1.36    | 1.32            | 1.26    | 1.31    | 0.05  | 5.53    | 3.77    | 4.20    | 5.18    | 2.68  |
| Co               | 0.72        | 1.01    | 0.55    | 0.76    | 0.23 | 2.27    | 1.37            | 1.90    | 0.47    | 5.57  | 5.95    | 4.77    | 4.20    | 4.75    | 6.07  |
| O-C-O            | 0.32        | 0.56    | 0.48    | 0.45    | 0.12 | 1.19    | 0.65            | 0.96    | 0.93    | 0.27  | 0.80    | 4.14    | 4.66    | 4.60    | 4.47  |
| Pt-N*            | 9.52        | 9.78    | 8.51    | 9.27    | 0.67 | 10.38   | 8.12            | 8.93    | 9.14    | 1.15  | 0.09    | 4.99    | 4.89    | 6.65    | 5.51  |
| Residual STD     | 1.51        | 1.51    | 1.26    | 1.60    | 1.03 | 1.26    | 1.26            | 1.26    | 1.25    | 1.16  | 1.17    | 1.38    | 1.38    | 1.38    | 1.38  |
|                  |             |         |         |         |      |         |                 |         |         |       |         |         |         |         |       |
| Ots              | 53.19       | 55.67   | 48.02   | 52.29   | 3.30 | 60.37   | 36.32           | 48.02   | 48.24   | 1.03  | 53.73   | 53.97   | 49.18   | 42.98   | 36.17 |
| C=O              | 39.78       | 40.64   | 45.62   | 42.01   | 3.15 | 33.20   | 61.02           | 45.62   | 46.61   | 13.94 | 45.80   | 42.10   | 46.23   | 51.58   | 36.71 |
| C=O aliphatic    | 6.46        | 3.69    | 6.35    | 5.50    | 1.57 | 6.42    | 2.66            | 5.32    | 5.13    | 2.14  | 0.48    | 3.93    | 4.59    | 5.43    | 4.64  |
| Ads O2/H2O       | 1.16        | 0.35    | 0.96    | 1.02    | 1.07 | 0.94    | 1.07            | 0.91    | 0.91    | 0.97  | 2.47    | 0.92    | 0.99    | 0.83    | 0.91  |
| Residual STD     |             |         |         |         |      |         |                 |         |         |       |         | 0.88    | 0.92    | 1.01    | 0.93  |
| Regions          | Sample1     | Sample2 | Sample3 | Average | STD  | Sample1 | Sample2         | Sample3 | Average | STD   | Sample1 | Sample2 | Sample3 | Average | STD   |
| Cts              | 98.34       | 97.73   | 97.47   | 97.85   | 0.45 | 95.17   | 95.92           | 96.48   | 95.86   | 0.54  | 88.33   | 88.20   | 88.39   | 88.67   | 89.58 |
| Ots              | 1.66        | 2.37    | 2.53    | 2.15    | 0.45 | 4.83    | 4.08            | 3.52    | 4.14    | 0.54  | 11.67   | 11.80   | 13.61   | 13.33   | 13.58 |

## XPS analysis.

**Table S1:** Deconvolution of High resolution XPS data

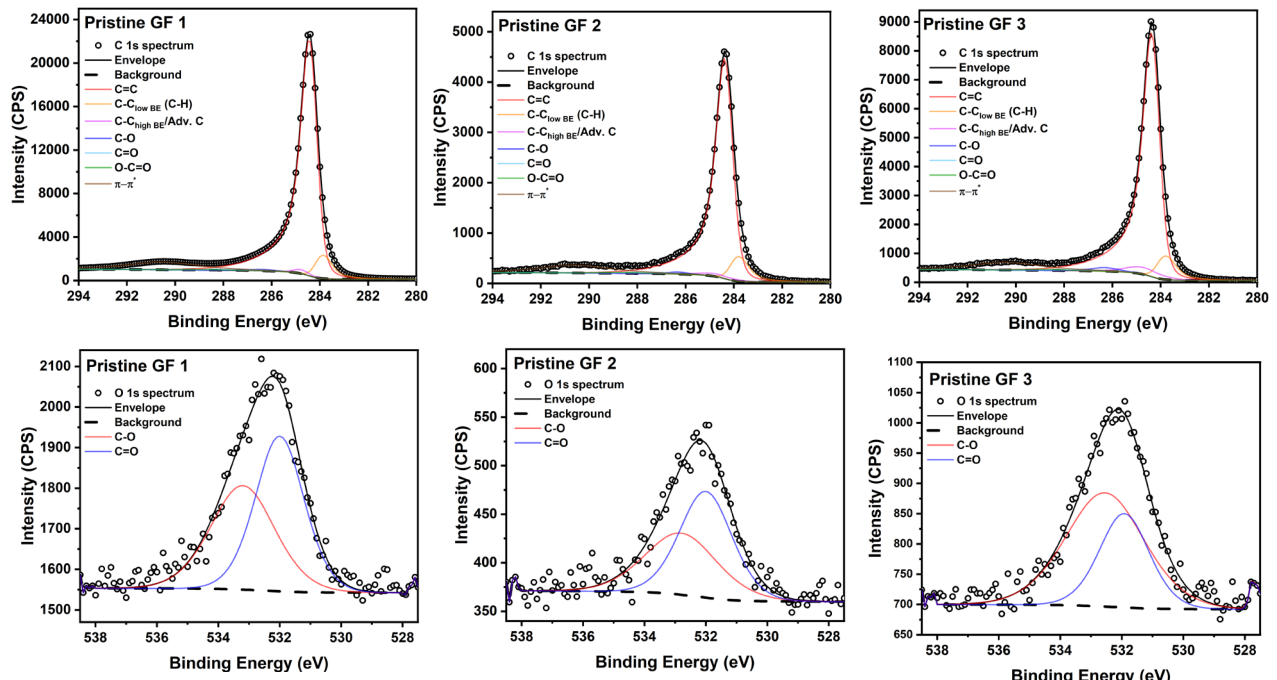


**Figure S1:** Pristine GF high resolution C1s & O1s spectra.

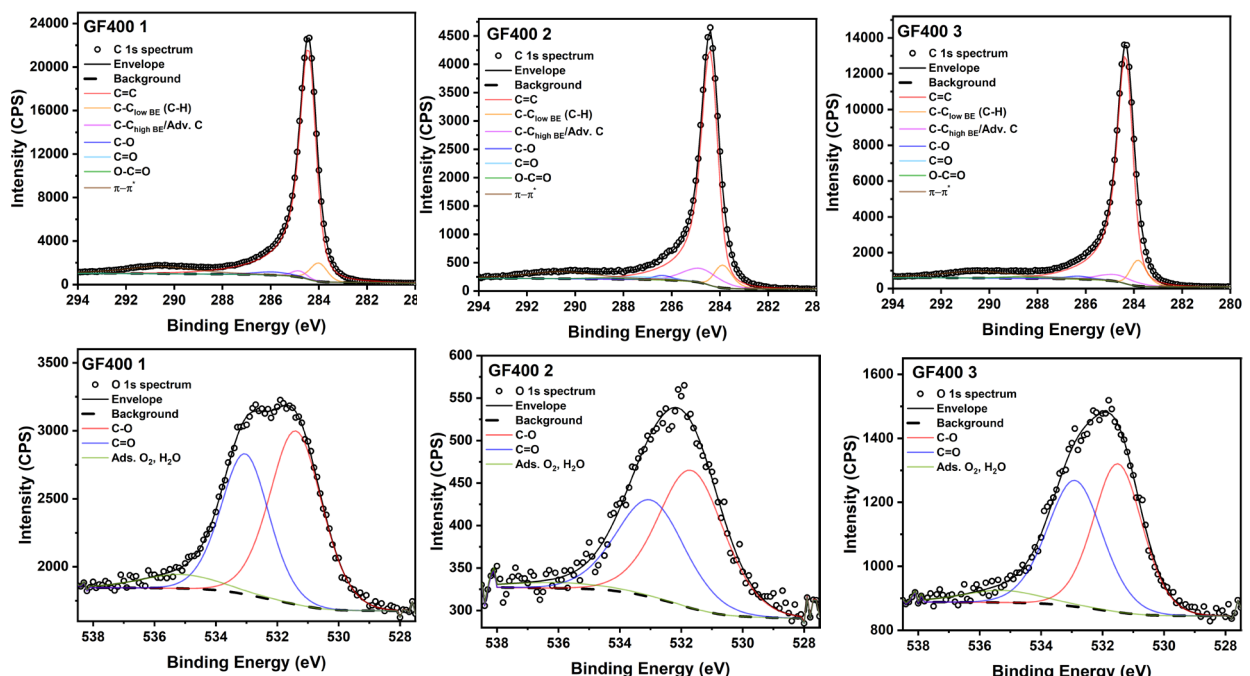


**Figure S2:** GF400 high resolution C1s & O1s spectra.

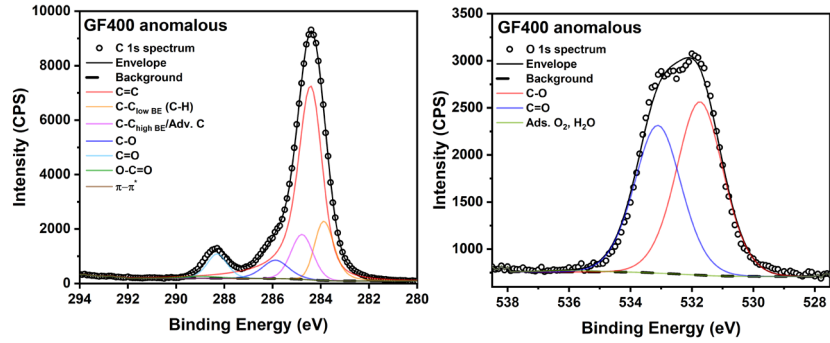


**Figure S3:** Anomalous GF400 high resolution C1s & O1s spectra.

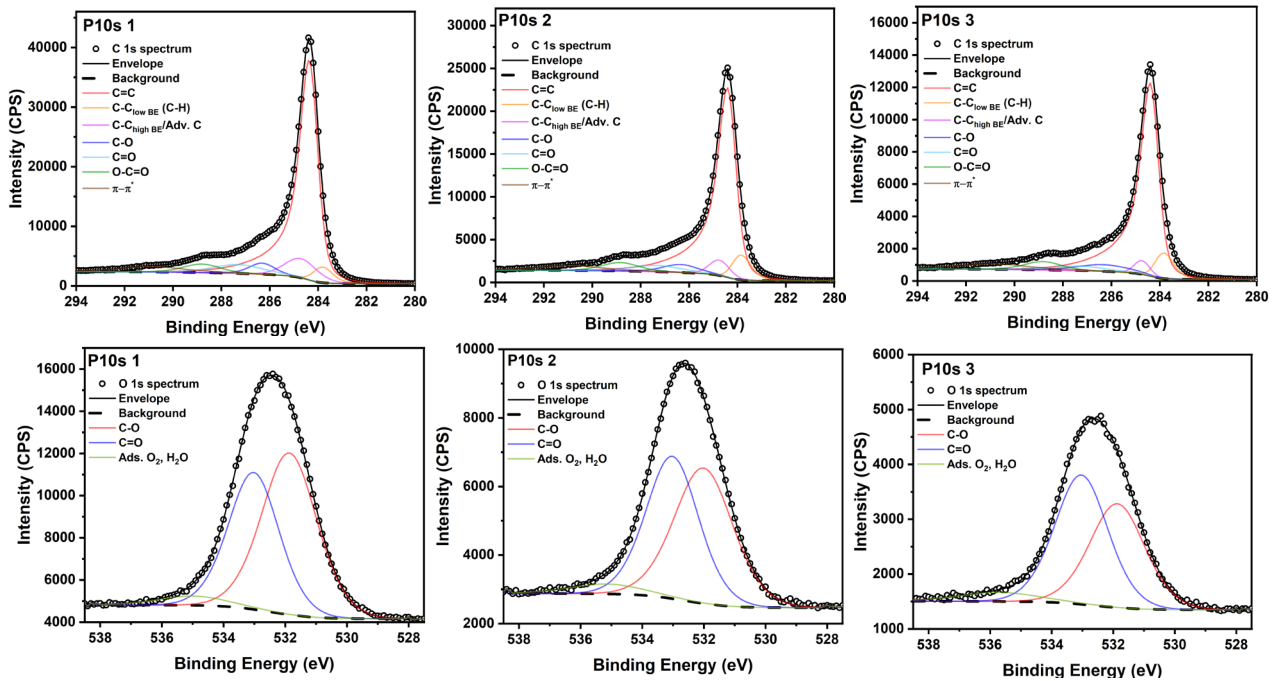


**Figure S4:** P10s high resolution C1s & O1s spectra.

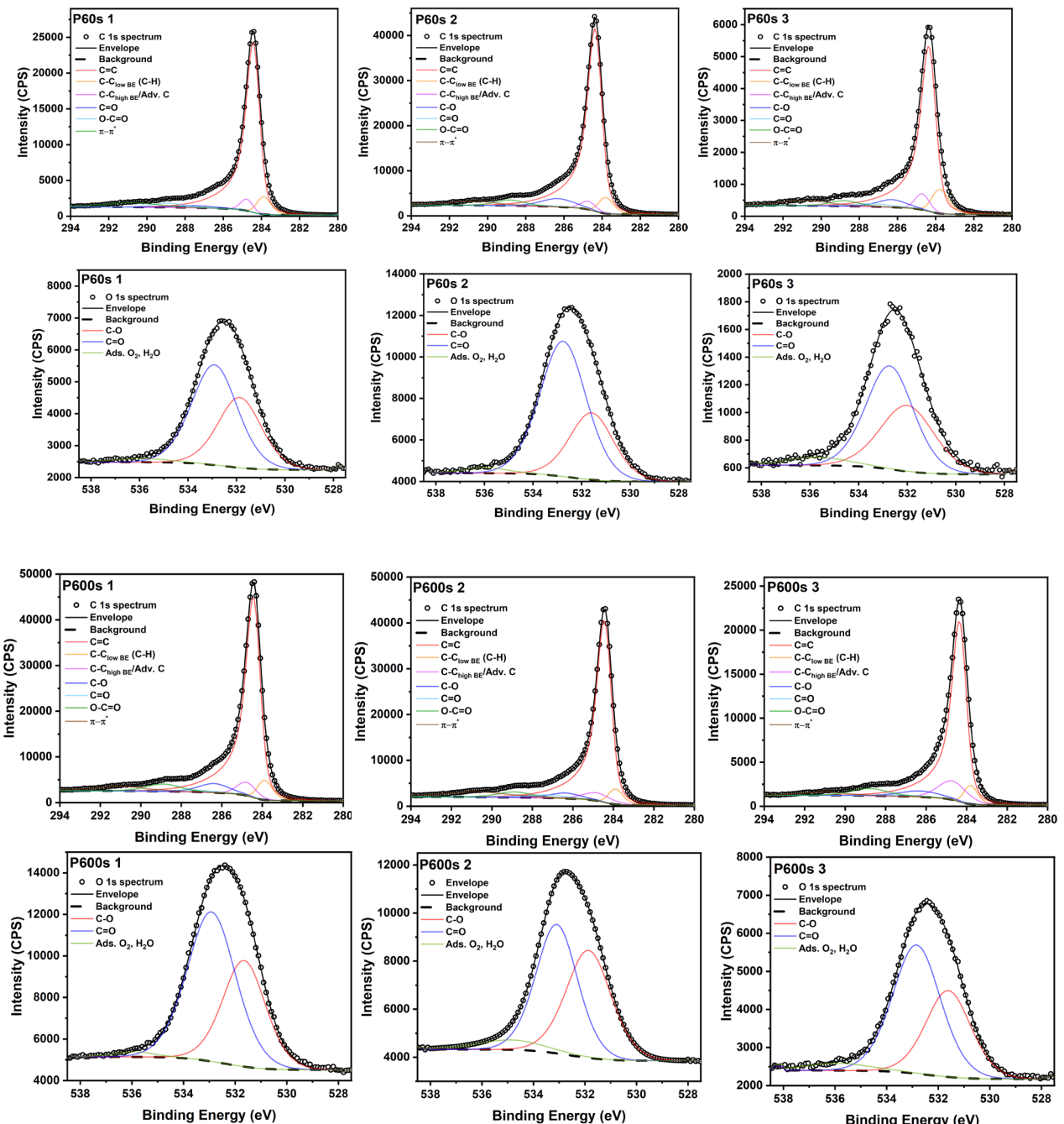


**Figure S6: P600s high resolution C1s & O1s spectra.**

## Raman analysis.

**Table S2:** Raman analysis including Gaussian and Lorentzian contributions for each band

| Pristine       | Id/Ig            | 2.679907518 | GF400          | Id/Ig            | 3.7135656687 | P10s           | Id/Ig            | 3.239609023    | P60s           | Id/Ig            | 3.283421792 | P600s          | Id/Ig            | 3.503555243    |
|----------------|------------------|-------------|----------------|------------------|--------------|----------------|------------------|----------------|----------------|------------------|-------------|----------------|------------------|----------------|
| <b>D1 band</b> |                  |             |                | <b>D1 band</b>   | Value        | Range          | <b>D1 band</b>   | Value          | <b>D1 band</b> | Value            | Range       | <b>D1 band</b> | Value            | Range          |
| Center         | 1332.14763       | 13200±1360  | Center         | 1333.94587       | 13200±1360   | Center         | 1333.57716       | 13200±1360     | Center         | 1332.5819        | 13200±1360  | Center         | 1333.638         | 13200±1360     |
| Area           | 289903.8301      |             | Area           | 432141.6882      |              | Area           | 254386.9861      |                | Area           | 482337.7709      |             | Area           | 224918.4845      |                |
| Gw             | 36.80391         | 5-60        | Gw             | 39.0275          | 5-60         | Gw             | 40.53759         | 5-60           | Gw             | 36.17939         | 5-60        | Gw             | 41.08113         | 5-60           |
| Lw             | 40               | 5-40        | Lw             | 40               | 5-40         | Lw             | 40               | 5-40           | Lw             | 40               | 5-40        | Lw             | 40               | 5-40           |
| FWHM           | <b>62.62825</b>  |             | FWHM           | <b>64.62409</b>  |              | FWHM           | <b>65.99181</b>  |                | FWHM           | <b>62.07194</b>  |             | FWHM           | <b>66.48632</b>  |                |
| Area %         | 65.51077466      |             | Area %         | 70.70440982      |              | Area %         | 62.83770222      |                | Area %         | 69.37630864      |             | Area %         | 64.20012701      |                |
| <b>G band</b>  |                  |             | <b>G band</b>  |                  |              | <b>G band</b>  |                  | <b>G band</b>  |                | <b>G band</b>    |             | <b>G band</b>  |                  | <b>G band</b>  |
| Center         | 1599.62903       | 1580±01610  | Center         | 1599.08449       | 1580±01610   | Center         | 1599.32798       | 1580±01610     | Center         | 1598.24704       | 1580±01610  | Center         | 1599.92889       | 1580±01610     |
| Area           | 1081.76.8039     |             | Area           | 116368.3965      |              | Area           | 78523.97752      |                | Area           | 146900.9471      |             | Area           | 64197.21366      |                |
| Gw             | 59.63946         | 5-60        | Gw             | 60               | 5-60         | Gw             | 59.91332         | 5-60           | Gw             | 60               | 5-60        | Gw             | 60               | 5-60           |
| Lw             | 8.90526          | 5-60        | Lw             | 6.26352          | 5-60         | Lw             | 5                | 5-60           | Lw             | 6.28942          | 5-60        | Lw             | 5                | 5-60           |
| FWHM           | <b>64.54405</b>  |             | FWHM           | <b>63.41925</b>  |              | FWHM           | <b>62.63135</b>  |                | FWHM           | <b>63.43338</b>  |             | FWHM           | <b>62.71811</b>  |                |
| Area %         | 24.44516246      |             | Area %         | 19.03949362      |              | Area %         | 19.39669317      |                | Area %         | 21.12927093      |             | Area %         | 18.32427993      |                |
| <b>D4 band</b> |                  |             | <b>D4 band</b> |                  |              | <b>D4 band</b> |                  | <b>D4 band</b> |                | <b>D4 band</b>   |             | <b>D4 band</b> |                  | <b>D4 band</b> |
| Center         | 1210             | 1190±01210  | Center         | 1210             | 1190±01210   | Center         | 1210             | 1190±01210     | Center         | 1210             | 1190±01210  | Center         | 1210             | 1190±01210     |
| Area           | 28893.98248      |             | Area           | 32756.92096      |              | Area           | 18721.27312      |                | Area           | 32050.27745      |             | Area           | 30638.71136      |                |
| Gw             | 57.69697         | 50-100      | Gw             | 161.39144        | 50-100       | Gw             | 139.3241         | 50-200         | Gw             | 129.30389        | 50-200      | Gw             | 88.9476          | 50-200         |
| Lw             | 200              | 50-200      | Lw             | 5                | 50-200       | Lw             | 5                | 50-200         | Lw             | 62.15468         | 50-200      | Lw             | 141.98034        | 50-200         |
| FWHM           | <b>216.43228</b> |             | FWHM           | <b>164.08122</b> |              | FWHM           | <b>142.01633</b> |                | FWHM           | <b>165.72796</b> |             | FWHM           | <b>186.70882</b> |                |
| Area %         | 6.52929393436    |             | Area %         | 5.3594894        |              | Area %         | 4.624457421      |                | Area %         | 4.609902177      |             | Area %         | 8.745431329      |                |
| <b>D3 band</b> |                  |             | <b>D3 band</b> |                  |              | <b>D3 band</b> |                  | <b>D3 band</b> |                | <b>D3 band</b>   |             | <b>D3 band</b> |                  | <b>D3 band</b> |
| Center         | 1510             | 1510±01530  | Center         | 1513.50276       | 1510±01530   | Center         | 1510             | 1510±01530     | Center         | 1510             | 1510±01530  | Center         | 1510             | 1510±01530     |
| Area           | 42824.71936      |             | Area           | 61065.86035      |              | Area           | 70299.72608      |                | Area           | 64389.82262      |             | Area           | 59604.4445       |                |
| Gw             | 100              | 5-100       | Gw             | 100              | 5-100        | Gw             | 150              | 5-150          | Gw             | 100              | 5-150       | Gw             | 150              | 5-150          |
| Lw             | 100              | 5-100       | Lw             | 100              | 5-100        | Lw             | 125.89049        | 5-150          | Lw             | 100              | 5-150       | Lw             | 96.37261         | 5-150          |
| FWHM           | <b>163.75859</b> |             | FWHM           | <b>163.75859</b> |              | FWHM           | <b>228.3376</b>  |                | FWHM           | <b>163.75859</b> |             | FWHM           | <b>208.08296</b> |                |
| Area %         | 9.677280009      |             | Area %         | 9.991226943      |              | Area %         | 17.36516898      |                | Area %         | 9.261410731      |             | Area %         | 17.01333226      |                |
| <b>D2 band</b> |                  |             | <b>D2 band</b> |                  |              | <b>D2 band</b> |                  | <b>D2 band</b> |                | <b>D2 band</b>   |             | <b>D2 band</b> |                  | <b>D2 band</b> |
| Center         | 1623.111865      | 1610±01630  | Center         | 1618.86937       | 1610±01630   | Center         | 1621.03663       | 1610±01630     | Center         | 1619.99649       | 1610±01630  | Center         | 1619.48278       | 1610±01630     |
| Area           | 10482.63493      |             | Area           | 38559.833526     |              | Area           | 11917.98331      |                | Area           | 36655.05744      |             | Area           | 13323.08427      |                |
| Gw             | 29.99223         | 5-50        | Gw             | 39.04722         | 5-50         | Gw             | 34.25234         | 5-50           | Gw             | 37.40419         | 5-50        | Gw             | 38.70923         | 5-50           |
| Lw             | 5                | 5-50        | Lw             | 5                | 5-50         | Lw             | 5                | 5-50           | Lw             | 5                | 5-50        | Lw             | 5                | 5-50           |
| FWHM           | <b>32.75537</b>  |             | FWHM           | <b>41.7895</b>   |              | FWHM           | <b>37.0043</b>   |                | FWHM           | <b>40.14951</b>  |             | FWHM           | <b>41.45211</b>  |                |
| Area %         | 2.368809148      |             | Area %         | 6.308927161      |              | Area %         | 2.943937212      |                | Area %         | 5.272223598      |             | Area %         | 3.802905325      |                |

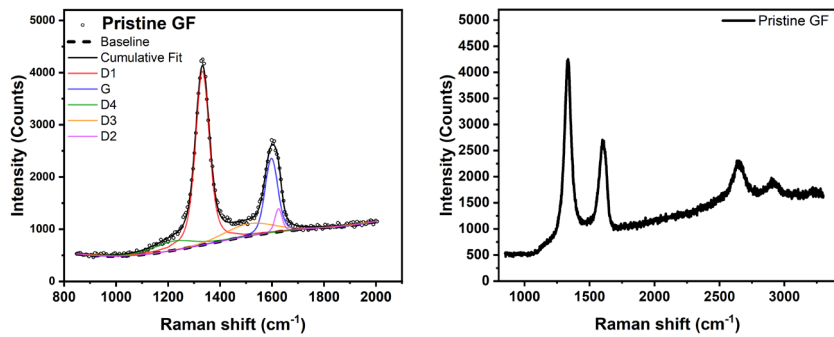


**Figure S7:** Pristine GF Raman spectrum and D/G band deconvolution.

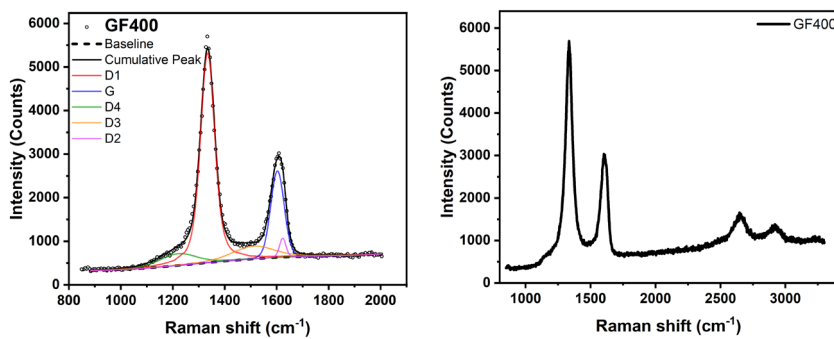


**Figure S8:** GF400 Raman spectrum and D/G band deconvolution.

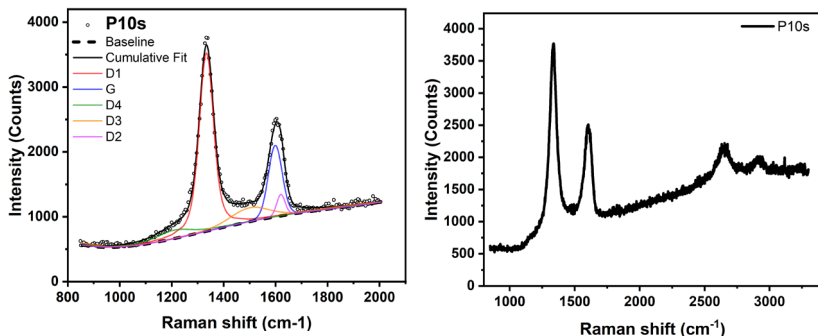


**Figure S9:** P10s Raman spectrum and D/G band deconvolution.

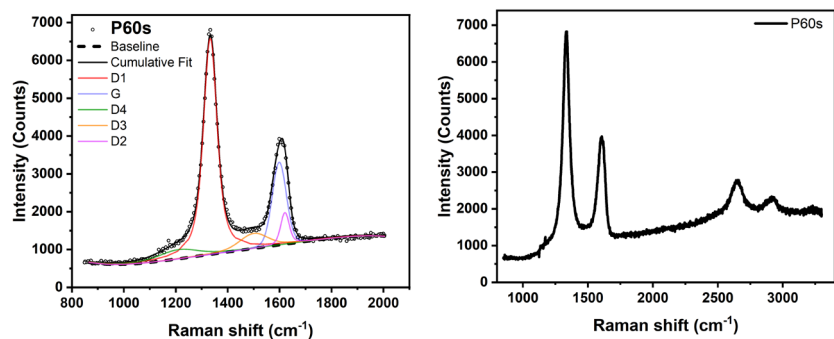


**Figure S10:** P60s Raman spectrum and D/G band deconvolution.

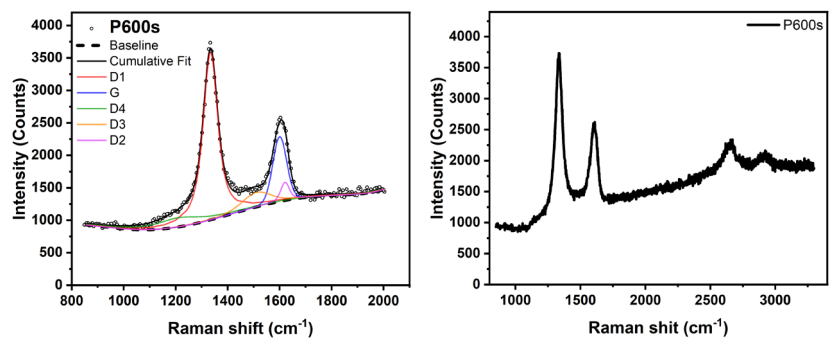


**Figure S11:** P600s Raman spectrum and D/G band deconvolution.

## Electrochemical double layer capacitance analysis

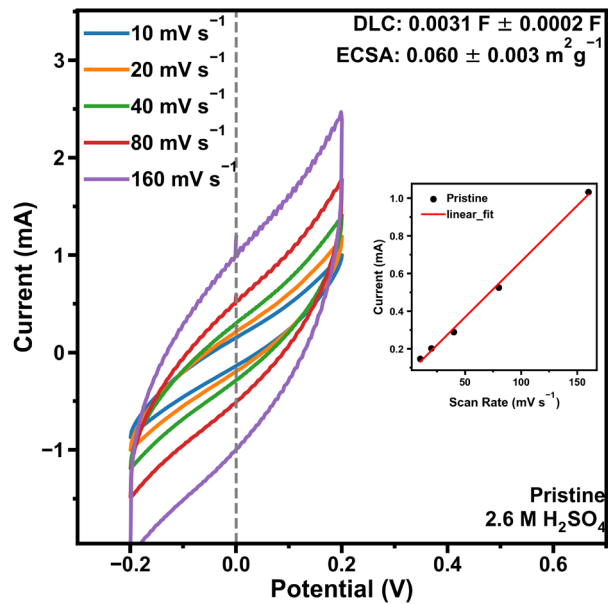


**Figure S12:** Pristine GF cyclic voltammetry showcasing non-faradaic current at different scan rates and linear fit of a current vs scan rate plot.

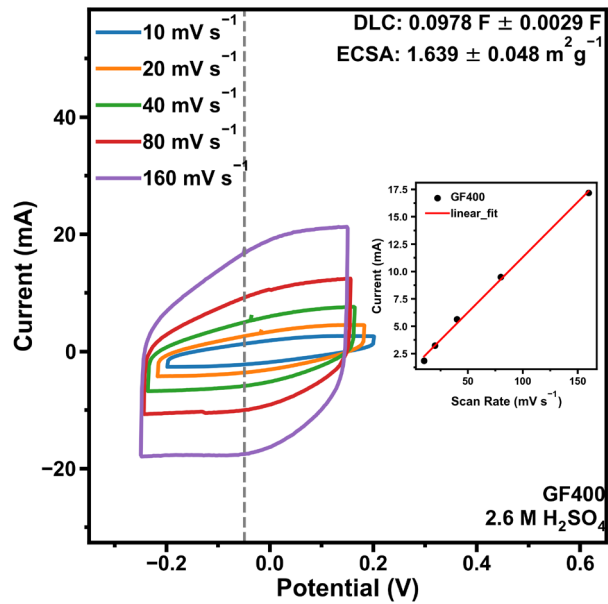


**Figure S13:** GF400 cyclic voltammetry showcasing non-faradaic current at different scan rates and linear fit of a current vs scan rate plot.

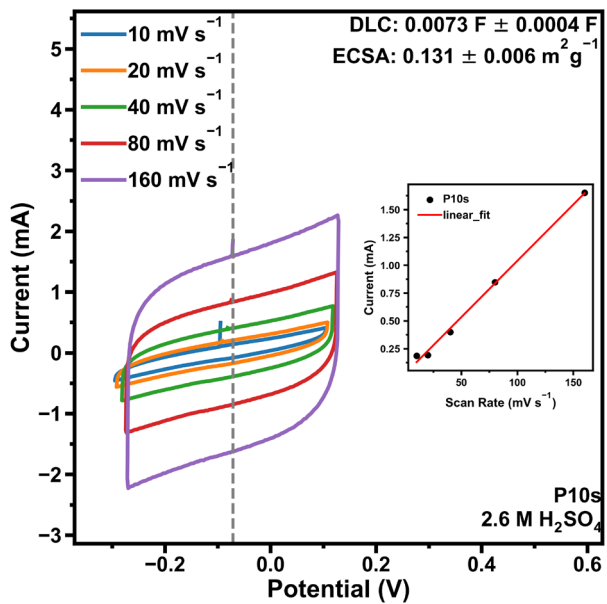


**Figure S14:** P10s cyclic voltammetry showcasing non-faradaic current at different scan rates and linear fit of a current vs scan rate plot.

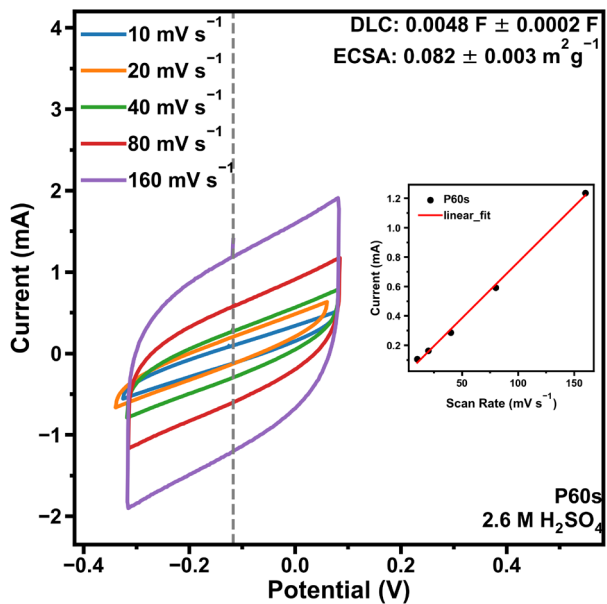


**Figure S15:** P60s cyclic voltammetry showcasing non-faradaic current at different scan rates and linear fit of a current vs scan rate plot.

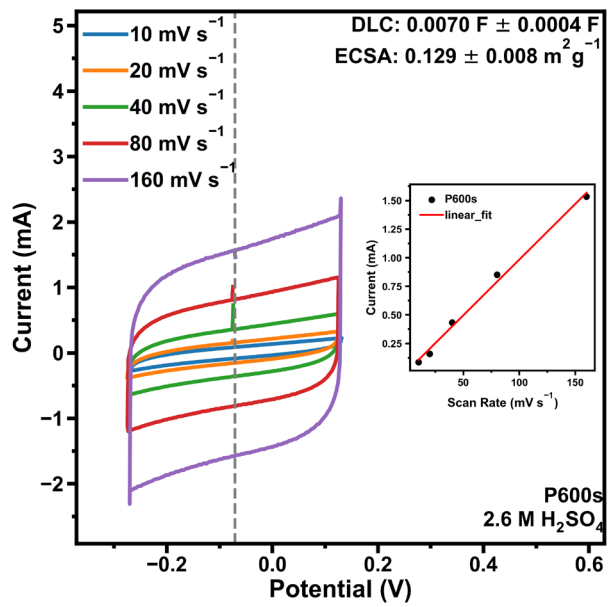


**Figure 16:** P60s cyclic voltammetry showcasing non-faradaic current at different scan rates and linear fit of a current vs scan rate plot.

## BET analysis.

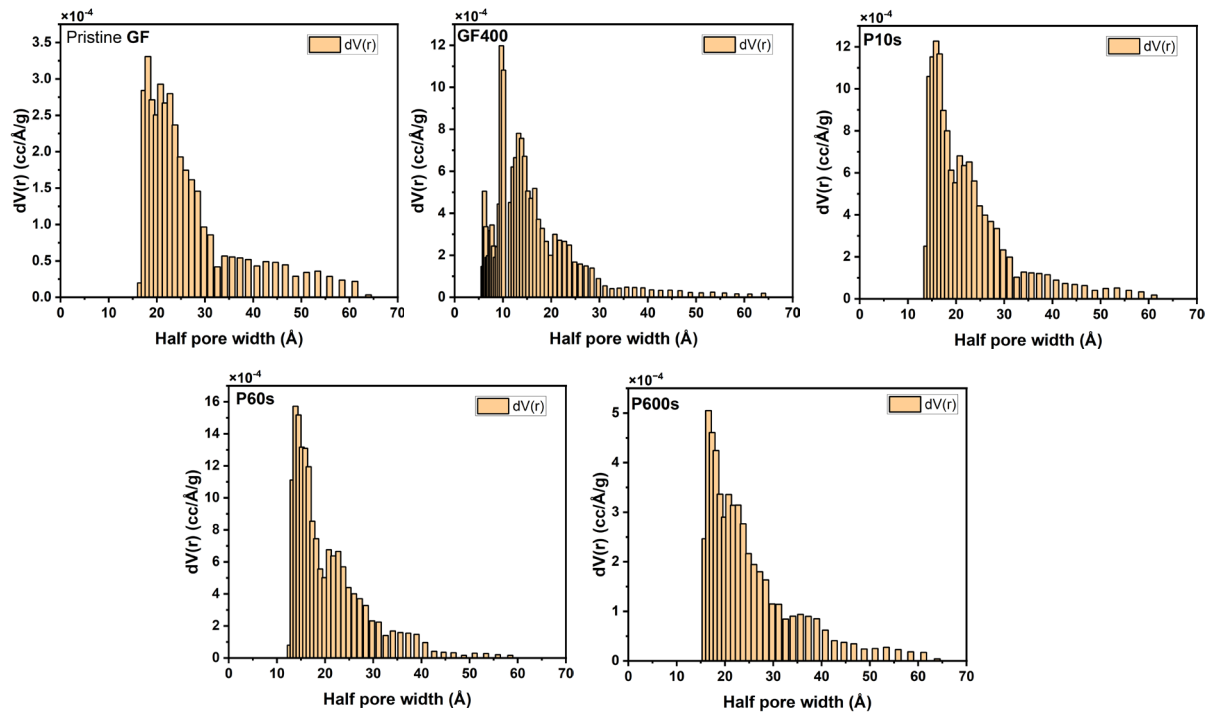


**Figure S17:** Pore-size distributions from electrodes as derived from BET analysis.

## Single-electrolyte cell analysis.

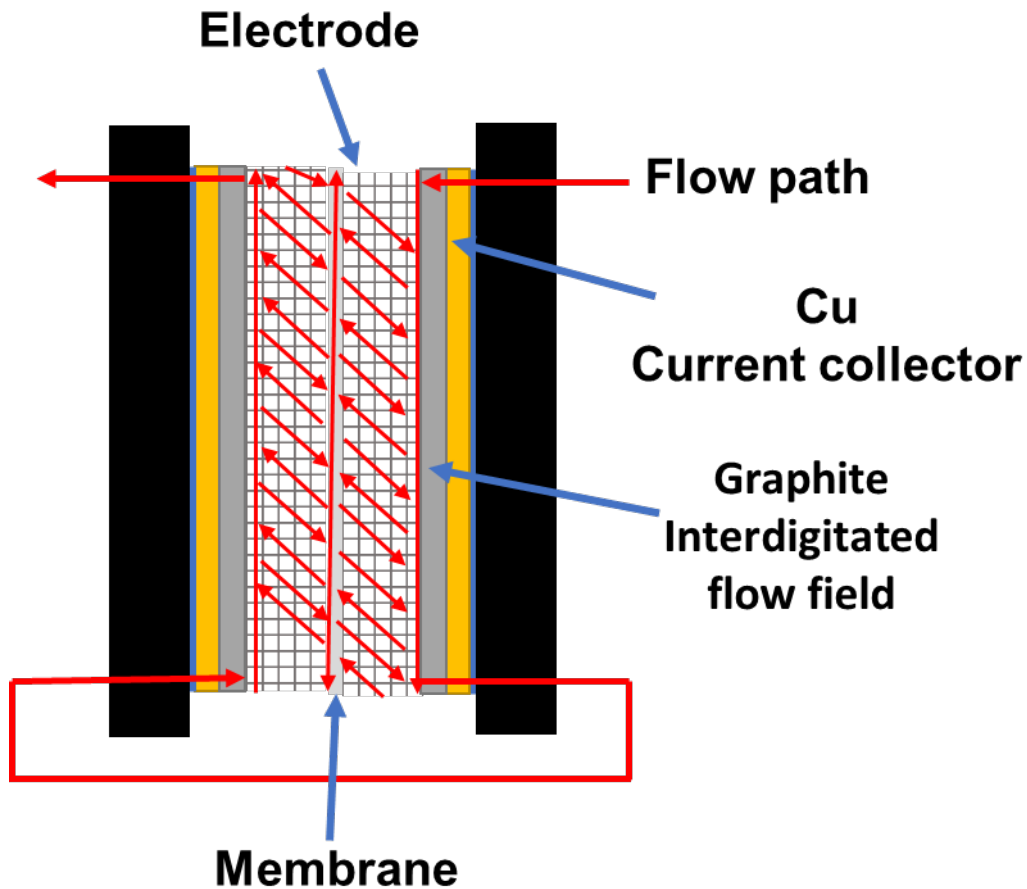


**Figure S18:** Schematic of a Single-electrolyte flow cell.

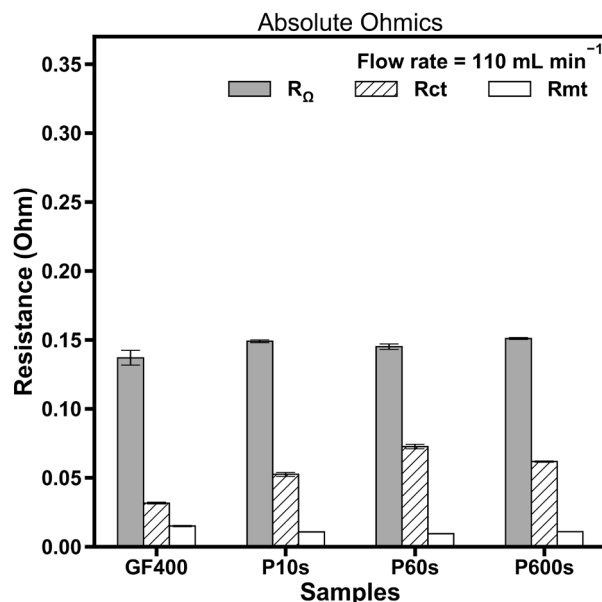


**Figure S19:** Breakdown of impedance contributions: Ohmic resistance (R<sub>s</sub>), charge-transfer resistance (R<sub>ct</sub>) and mass-transport resistance (R<sub>m</sub>) at 110 mL min<sup>-1</sup>

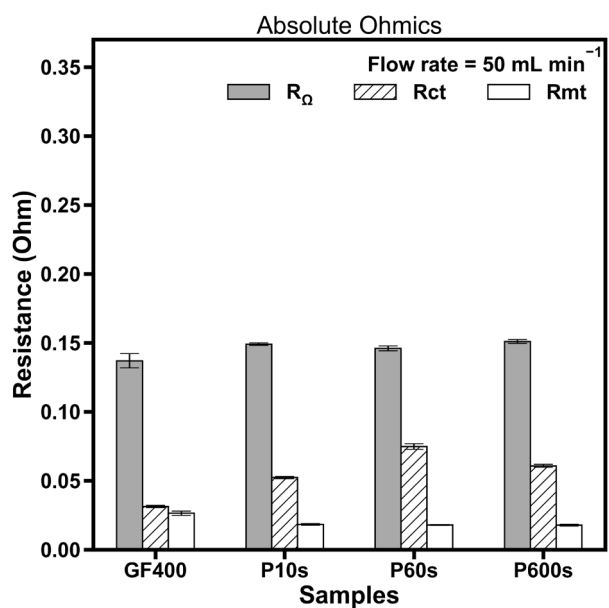


**Figure S20:** Breakdown of impedance contributions: Ohmic resistance ( $R_s$ ), charge-transfer resistance ( $R_{ct}$ ) and mass-transport resistance ( $R_{mt}$ ) at  $50 \text{ mL min}^{-1}$

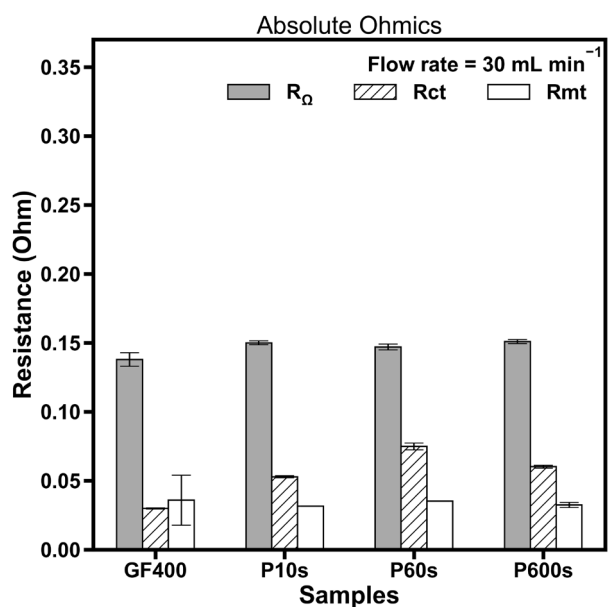


**Figure S21:** Breakdown of impedance contributions: Ohmic resistance ( $R_s$ ), charge-transfer resistance ( $R_{ct}$ ) and mass-transport resistance ( $R_{mt}$ ) at  $30 \text{ mL min}^{-1}$

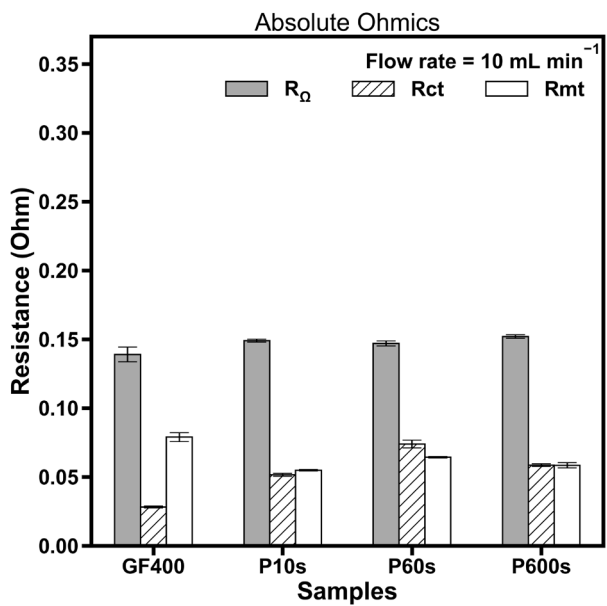


**Figure S22:** Breakdown of impedance contributions: Ohmic resistance ( $R_s$ ), charge-transfer resistance ( $R_{ct}$ ) and mass-transport resistance ( $R_{mt}$ ) at  $10 \text{ mL min}^{-1}$

## Pressure drop analysis.

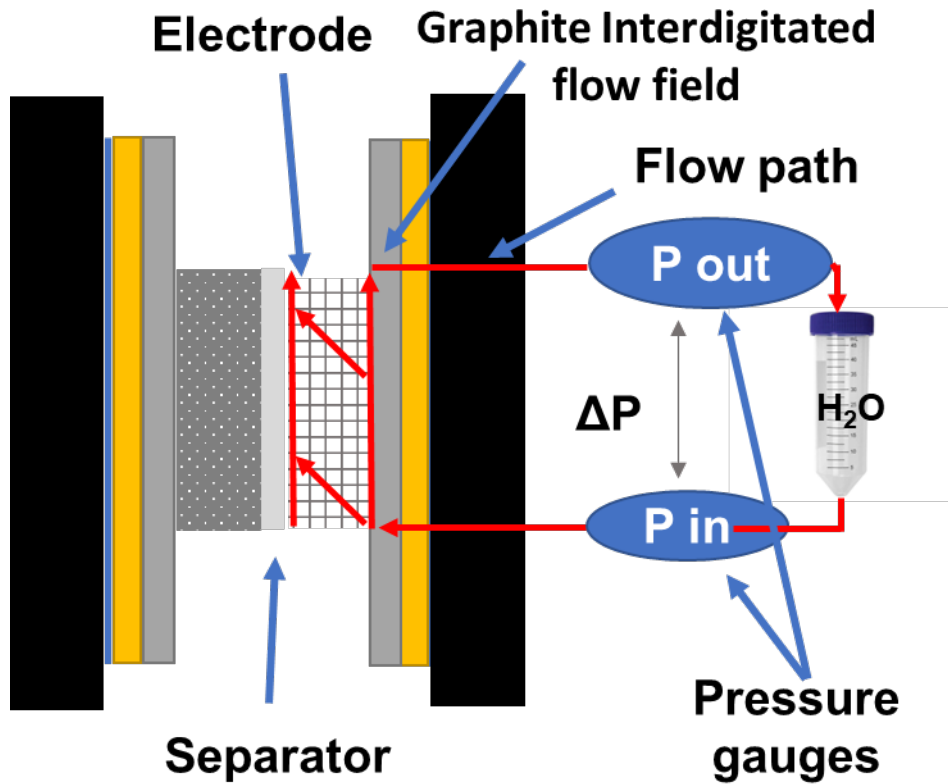


**Figure S23:** Schematic of a Flow cell set up to perform pressure drop measurements.

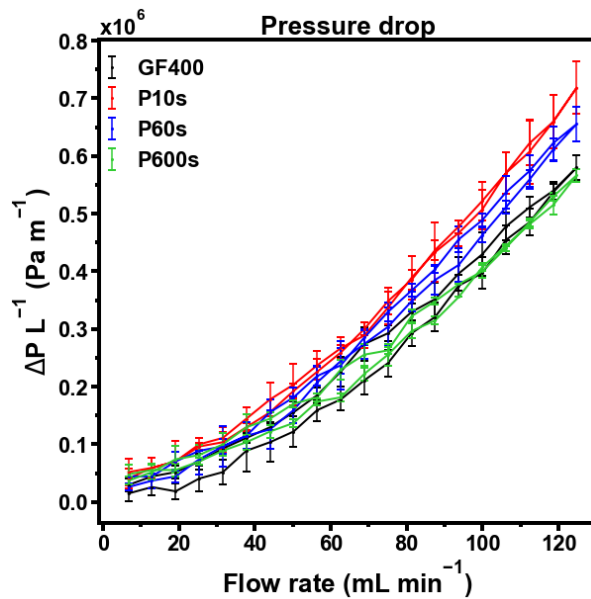


**Figure S24:** Pressure drop plot from different electrodes showcasing curve hysteresis.

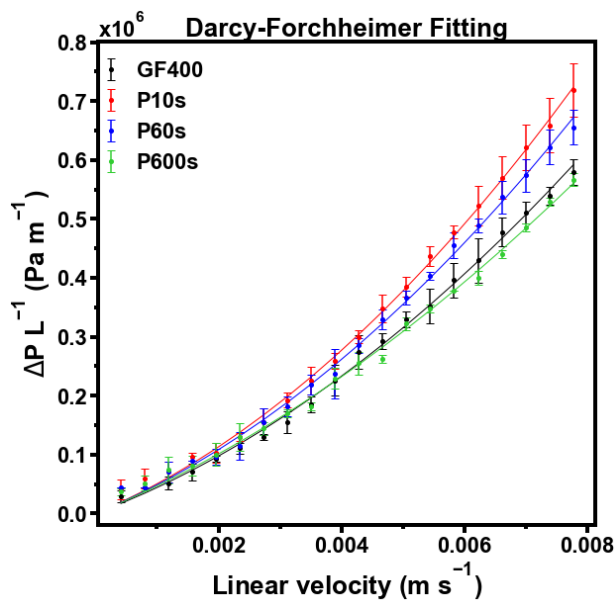


**Figure S25:** Darcy-Forchheimer fitting.

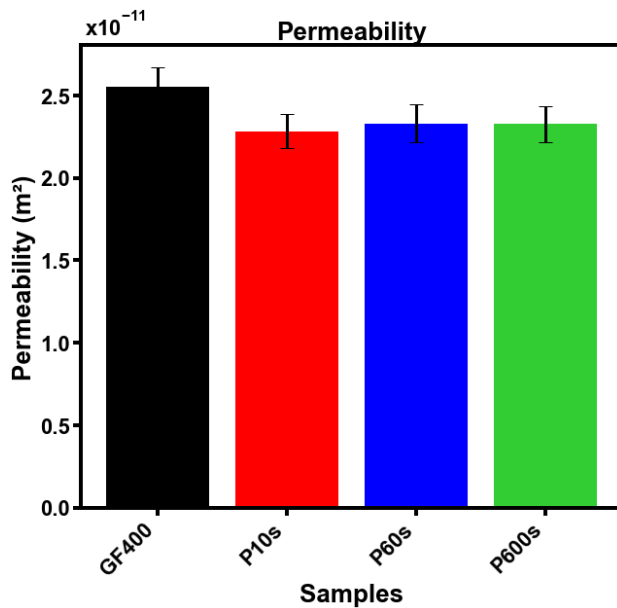


**Figure S26:** Permeability values derived from Darcy-Forchheimer fitting